



Network Pharmacology and Molecular Docking Studies of Ethnopharmacological Plants from Sulawesi as Antidiabetics

Muhammad Sulaiman Zubair¹, Yonelian Yuyun¹, Waode Sitti Musnina¹, Ahmad Najib², Firzan Nainu³, Muhammad Arba⁴, Dwi Rahmi Paneo¹, Ersanda Nurma Praditapuspa⁵, Saipul Maulana^{1*}

¹Department of Pharmacy, Faculty of Science, Tadulako University, Palu, Indonesia

²Department of Pharmacy, Faculty of Pharmacy, Indonesia Muslim University, Makassar, Indonesia

³Department of Pharmacy, Faculty of Pharmacy, Hasanuddin University, Makassar, Indonesia

⁴Department of Pharmacy, Faculty of Pharmacy, Halu Oleo University, Kendari 93232, Indonesia

⁵Department of Pharmacy, Faculty of Pharmacy, Universitas Hang Tuah, Surabaya 60111, Indonesia

ARTICLE INFO

Article history:

Received 27 December 2024

Revised 31 December 2024

Accepted 09 February 2025

Published online 01 April 2025

ABSTRACT

Diabetes is a degenerative disease affecting many people in Indonesia, where herbal preparations offer an alternative treatment. This study aims to identify potential antidiabetic drugs from four ethnopharmacological plants of Sulawesi (*Cordia myxa* L., *Syzygium cumini*, *Syzygium malaccense*, and *Antidesma bunius*) using network pharmacology and molecular docking approaches. Secondary metabolites in the ethanolic extracts were identified using gas chromatography-mass spectrophotometry (GC-MS), followed by analysis of potential antidiabetic targets through network pharmacology and docking studies with Molecular Operating Environment (MOE) software. Network pharmacology revealed PPAR γ as a potential target for *C. myxa* and GCG receptors for the other plants. Docking analysis showed that *C. myxa* compounds bind strongly to PPAR γ (PDB ID: 5YCP), surpassing Rosiglitazone (-7.49635 kcal/mol), with top binding energies observed for Squalane (-9.6078 kcal/mol), 2,6,10,14,18,22-Tetracosahexaene, 2,6,10,15,19,23-hexamethyl-(all-E)- (-8.7069 kcal/mol), and Anodendroside G monoacetate (-8.0845 kcal/mol). Meanwhile, for GCG (PDB ID: 5EE7) receptor interactions, several compounds demonstrated stronger binding than MK-0893 (-5.66941 kcal/mol). *A. bunius* exhibited the highest GCG binding affinities from terpenoid of 2,5,7,8-Tetramethyl-2-(4,8,12-Trimethyltridecyl)-3,4-Dihydro-2h-Chromen-6-Yl Hexofuranoside (-8.8001 kcal/mol), while *S. malaccense* and *S. cumini* compounds showed moderate to strong binding energies ranging from -7.6398 to -6.5939 kcal/mol. These findings highlight the significant antidiabetic potential of *C. myxa* targeting PPAR γ and *A. bunius*, *S. malaccense* and *S. cumini* targeting GCG receptors, offering promising candidates for antidiabetic drug development.

Copyright: © 2025 Zubair *et al.* This is an open-access article distributed under the terms of the [Creative Commons Attribution License](https://creativecommons.org/licenses/by/4.0/), which permits unrestricted use, distribution, and reproduction in any medium, provided the original author and source are credited.

Keywords: *Ethnopharmacological plants, Gas Chromatography-Mass Spectrometry, Molecular docking, Network pharmacology, Diabetes Mellitus*

Introduction

Diabetes mellitus (DM) is a prevalent global health issue, including in Indonesia. According to the International Diabetes Federation (IDF), the prevalence of DM has been rising significantly since 2015 and is projected to reach 6.16 billion by 2040. DM comprises a group of chronic metabolic disorders characterized by hyperglycemia, resulting from defects in insulin production, insulin action, or both¹. The majority of DM cases are type II. Management of type II DM involves both non-pharmacological and pharmacological therapies. Non-pharmacological approaches focus on lifestyle modifications, while pharmacological treatments involve the use of oral anti-diabetic

medications². However, long-term use of synthetic antidiabetic drugs, such as acarbose, can lead to side effects, including nausea, vomiting, abdominal pain, and bloating, affecting the digestive system^{3, 1}. Consequently, natural medicine is increasingly considered an alternative therapy due to its potential benefits and minimal side effects. Previous studies have identified several ethnopharmacological plants from Sulawesi, including *C. myxa* L.⁴⁻⁶, *S. cumini*^{7,8}, *S. malaccense*⁹⁻¹¹, and *A. bunius*^{6,12,13}, as potential candidates for antidiabetic drug development. These studies have explored the biological activities and chemical compounds of these plants. For instance, ELISA studies on the leaf extract of *C. myxa* L. have demonstrated α -glucosidase inhibitor activity⁴. Additionally, an in silico approach has been employed to screen compounds from *C. myxa* L. with potential as α -glucosidase inhibitors⁵. Furthermore, mapping studies of active compounds in the n-hexane fraction of *C. myxa* L. leaves, along with postprandial bioassays and radical scavenging activity assessments¹⁴, have indicated the plant's potential antidiabetic and antioxidant properties.

The experimental findings have conclusively demonstrated the therapeutic potential of these plant species. To comprehensively understand the molecular basis of these therapeutic effects, a multi-tiered analytical approach has been implemented. Initially, metabolomic profiling utilizing gas chromatography-mass spectrometry (GC-MS) approach has enabled the detailed characterization of tentative bioactive metabolites through identification and quantification by splitting ions that produce typical fragmentation patterns of parent ions¹⁵. Moreover, the identified

*Corresponding author. E mail: saifulmaulana011@gmail.com

Tel: +62 822-9348-2860

Citation: Zubair MS, Yuyun Y, Musnina WS, Najib A, Nainu F, Arba M, Paneo DR, Praditapuspa EN, Maulana S. Network Pharmacology and Molecular Docking Studies of Ethnopharmacological Plants from Sulawesi as Antidiabetics. Trop J Nat Prod Res. 2025; 9(3): 1123 -1135 <https://doi.org/10.26538/tjnpr/v9i3.30>

Official Journal of Natural Product Research Group, Faculty of Pharmacy, University of Benin, Benin City, Nigeria

compounds were subsequently analyzed through Network Pharmacology (NP), a sophisticated computational framework that systematically maps and analyzes the intricate web of interactions between plant-derived compounds and their corresponding biological targets simultaneously interact with various cellular proteins and signaling pathways, offering insights into their mechanisms of action at the molecular level¹⁶. The system biology perspective has proven particularly valuable in understanding the pleiotropic effects of natural products, as demonstrated by our previous study demonstrating the anti-inflammatory properties of phenolic acid derivatives through their specific inhibitory action on TNF- α convertase receptors¹⁷. Subsequent validation of these promising therapeutic candidates was conducted through molecular docking simulations that enable precise prediction and visualization of binding interactions. Our previous studies have demonstrated that the docking method effectively identified anticancer bioactive compounds from *Begonia medicinalis* plant by utilizing the virtual screening method of the Begonia genus plant compounds database¹⁸⁻²⁰. Similarly, the discovery of antidiabetic compounds has been achieved through molecular docking approaches, exemplified by compounds from *Ficus lutea* plants²¹. Furthermore, inhibitor compounds for the 3CL-protease enzyme of SARS-CoV-2 were successfully identified from *Zingiber officinale* plants using a GC-MS-based molecular docking approach²². Therefore, in this study, we performed network pharmacology to identify the potential antidiabetic target from four ethnopharmaca plants of Sulawesi and then further validated the potency by molecular docking of plants metabolites compounds on the specific antidiabetic protein target.

Materials and Methods

Plant Materials

The leaves of *Cordia myxa* L. (voucher specimen no. 117.CM.05.2024) were collected on May 21, 2024, from Rante Padang-Rante Mario Village, Malua District, Enrekang Regency, South Sulawesi, Indonesia (3°22'26"S; 119°53'15"E). Similarly, the leaves of *Syzygium cumini* (voucher specimen no. 118.SC.05.2024), *Syzygium malaccense* (voucher specimen no. 119.SM.05.2024), and *Antidesma bunius* (voucher specimen no. 120.AB.05.2024) were obtained on the same date from Kelarembeng Village, Bontonompo District, Gowa Regency, South Sulawesi, Indonesia (5°18'21"S; 119°23'48"E). The taxonomic identification of all plant species was conducted by the Botanical Division of the Pharmacognosy-Phytochemistry Laboratory, Faculty of Pharmacy, Universitas Muslim Indonesia.

Preparation of plant material and extraction

Each fresh leaf sample was carefully cleaned to remove debris and air-dried at room temperature for one week. Subsequently, 300 g of the dried material from each species was finely ground into a powder using a traditional grinder. The powdered leaf samples were extracted using the maceration method, with 10 liters of 95% ethanol serving as the organic solvent. The maceration process was carried out over a period of 3-5 days at room temperature, during which the mixture was intermittently stirred to ensure thorough extraction. After the maceration period, the resulting mixture was filtered to separate the liquid extract from the solid residue. The residue was re-soaked under the same conditions, and this process was repeated three times to maximize the extraction yield. The combined filtrates from each repetition were evaporated under reduced pressure using a rotary evaporator to remove the solvent, yielding a viscous ethanolic extract. These extracts were then stored under appropriate conditions for further analysis.

GC-MS Analysis

Ethanol extracts of each plant leaves were analyzed by GC-MS (Shimadzu QP-2010 Gas Chromatograph Mass Spectrometer Ultra), equipped by an autosampler AOC-20i and capillary column (SH-Rxi-5Sil MS) with the diameter 30 m x 0.25 mm x 0.25 mm. Helium was used as carrier gas (1.0 mL/min). Temperature injection of 250°C; splitless mode; a column oven temperature of 70°C at the beginning and held for 2 min, then ramped to 200°C at the rate of 10°C/min and end temperature 280°C and held for 9 min at the rate 5°C/min; an MS ion

source temperature of 200°C, and an interface temperature of 280°C were set. The secondary metabolites were identified by comparing the experimental molecular mass spectra and base peak of each chromatogram with the Wiley and NIST database libraries²³.

Network Pharmacology

Identification of Gene Targets Associated Active Compounds

The identification of potential gene targets was based on the active compounds derived from GC-MS analysis. The pharmacological activities of these genetic targets were predicted using SMILES data, which was later integrated into SwissTargetPrediction (<http://www.swisstargetprediction.ch/>) database. The compilation of genetic targets was standardized according to the guidelines established by the HUGO Gene Nomenclature Committee (HGNC). This standardization process utilized the Uniprot database (<https://www.uniprot.org/id-mapping>) to rectify any discrepancies in gene nomenclature across different databases^{24,25}.

Identification of Gene Targets Related with Diabetes

The identification of target proteins involved in the pathogenesis of cervical cancer was conducted through an extensive search of multiple genomic databases, including Gene Expression Omnibus (GSE) (GSE184050) (<https://www.ncbi.nlm.nih.gov/geo/>), Online Mendelian Inheritance in Man (OMIM) (<https://omim.org/>), GeneCards (<https://www.genecards.org/>), DrugBank (<https://go.drugbank.com/>), DisGeNET (<https://disgenet.com/>), and PharmGKB (<https://www.pharmgkb.org/>). These resources were utilized to gather relevant information on genes and proteins associated with diabetes by employing keywords such as "diabetes," "type 2 diabetes mellitus," and "T2DM". After collecting the data, the target proteins were standardized according to the UniProt database, following a methodology similar to that used in previous steps²⁴⁻²⁶.

Construction of Protein-protein interaction (PPI) network and enrichment analysis

An interaction network was developed to explore the relationships between genes associated with plant-derived active compounds and target proteins associated to diabetes, utilizing the STRING database with a high confidence threshold of 0.700 and a false discovery rate (FDR) stringency of 5%. The resulting protein networks were subsequently analyzed using Cytoscape 3.9.1 software. This visualization of protein-protein interaction (PPI) networks enabled the identification of similar genes among the targets. In this network, each protein's topological identity is represented as a "node," while the interactions between genes and proteins are denoted as "edges." Further analysis of this network included metrics such as degree, betweenness, and centrality (BC). Nodes with high degree values, indicating the highest-ranked target proteins, are regarded as playing crucial roles within the PPI network. To gain insights into the biological functions of these proteins, an enrichment analysis was performed using MetaScape (<https://metascape.org/>), WebGestalt (<https://webgestalt.org/>), and Enrichr (<https://maayanlab.cloud/Enrichr>)²⁷⁻²⁹.

Molecular docking

In this study, the receptor associated with *diabetes mellitus* was analyzed based on network pharmacology. To determine which test compounds exhibited superior binding stability, molecular docking procedures were conducted using the Molecular Operating Environment (MOE) software (version 2020). The crystal structures of the receptors were initially refined by adding hydrogen atoms and protonating them. Following this, the AMBER 99 force field was applied to minimize the energy of the macromolecules prior to docking simulations. The test compounds were first constructed in two dimensions using ChemDraw software (version 19.1, Perkin Elmer Informatics) and then imported into the MOE database. These 2D structures were converted into three-dimensional conformations by adding both polar and nonpolar hydrogen atoms, followed by optimization using the MMFF94x force field. The docking process facilitated the analysis of potential interactions within the receptor's active site, with docking coordinates selected based on the binding pose of the native ligand. To validate the docking protocol, post-docking

results for the native ligand were assessed by calculating the Root Mean Square Deviation (RMSD) in comparison to its original conformation; a valid docking protocol is indicated by an RMSD value below 2 Å. Furthermore, the stability of ligand-receptor interactions—encompassing both native ligands and test compounds—was evaluated using S Score, which reflects binding energy. Lower binding energy values indicate better stability of interactions among the compounds³⁰.

Results and Discussion

Extraction and GC-MS Analysis of Plants Ethanolic Extracts

The extraction of each plant obtained the viscous ethanol extract of *C. myxa*, *A. bunius*, *S. malaccense*, and *S. cumini* with the yields of 1.93%, 2.28%, 2.97% and 1.87%, respectively. Gas Chromatography-Mass Spectrometry (GC-MS) analysis of each extracts revealed the presence of diverse metabolite compounds across several species. The analysis identified 88 distinct metabolites in *C. myxa*, while *A. bunius* contained 95 compounds. *S. malaccense* yielded 71 compounds, and *S. cumini* demonstrated the highest number with hundred metabolite compounds. In this study, *C. myxa*, *A. bunius*, *S. malaccense*, and *S. cumini* exhibited distinct metabolite compositions, with *A. bunius* showing the highest number of terpenoids compounds followed by *S. cumini* and *S. malaccense*. Meanwhile, *C. myxa* showing the highest number of fatty acids compounds which aligns with previous research that underscores the utility of GC-MS in plant metabolomics, particularly in revealing variations in metabolite profiles across different species (Figure 1).

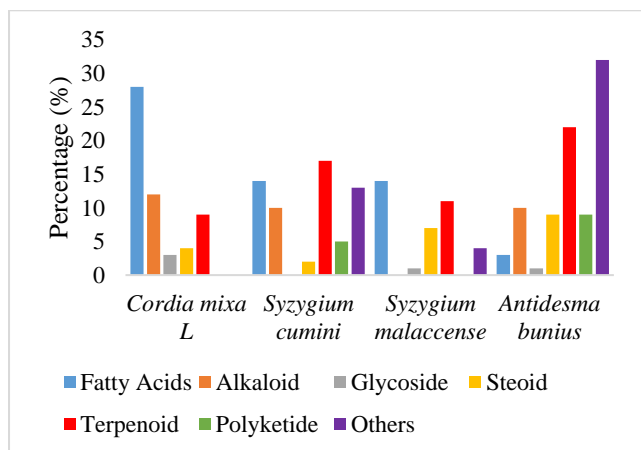


Figure 1: Tentative phytoconstituents profile of *C. myxa*, *A. bunius*, *S. malaccense*, and *S. cumini* extracts identified by GC-MS.

The distinct clustering patterns observed in metabolite profiles across various plant families suggest that genetic and environmental factors significantly influence metabolite production. This is corroborated by findings from a study that explored the metabolic diversity among different plant families, revealing that similar biosynthetic pathways often lead to analogous metabolite classes within related species³¹.

Network Pharmacology

The SwissTarget database analysis revealed significant variations in compound-gene interactions across the four medicinal plants. *S. cumini* demonstrated the highest number of interactions with 1,132 genes, substantially higher than *S. malaccense* (906 genes), *A. bunius* (804 genes), and *C. myxa L* (662 genes). The diabetes-associated gene analysis across multiple databases identified GSE as the primary database with 1,743 genes, followed by DisGeNET (318 genes), OMIM (260 genes), DrugBank (139 genes), PharmGKB (55 genes), and GeneCards (53 genes) (Figure 2). The multi-database approach provides comprehensive validation of the potential therapeutic targets in diabetes treatment.

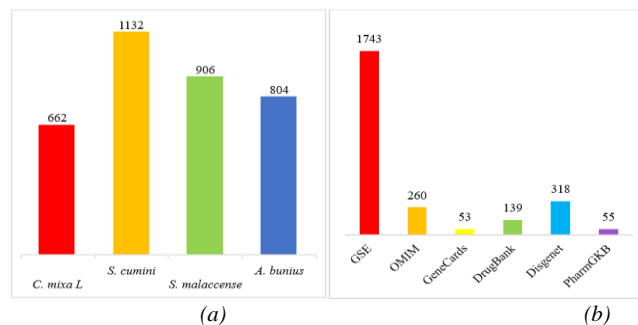


Figure 2: Number of genes related to compound structures from the SwissTarget database (a) and the number of genes associated with diabetes mellitus across multiple databases (b).

The STRING database visualization analysis revealed complex interaction patterns, with degree measurements indicating the quantity of direct nodal connections in the network. In *C. myxa L*, PPARG displayed the highest connectivity score of 20, establishing its significance as a central hub protein in anti-diabetic mechanisms. This was complemented by PPARA showing 17 connections, while RXRA exhibited 8 interconnections (Figure 3A & (20 interactions) correlating with extensive biological process involvement, showing maximum counts (15) across metabolic processes, stimulus response, and biological regulation (Figure 4A). This aligns with research 37 demonstrating PPARG's crucial role in modulating multiple synchronized glucose homeostasis regulation³⁹. *A. bunius* showed moderate but significant enrichment (13 counts) across (Table 1). The network analysis of *S. cumini* revealed GCG as a prominent node with 16 interactions, accompanied by SLC5A2 and DPP4, each demonstrating 9 network connections (Figure 3B & (20 interactions) correlating with extensive biological process involvement, showing maximum counts (15) across metabolic processes, stimulus response, and biological regulation (Figure 4A). This aligns with research 37 demonstrating PPARG's crucial role in modulating multiple synchronized glucose homeostasis regulation³⁹. *A. bunius* showed moderate but significant enrichment (13 counts) across (Table 1). *A. bunius* showed comparable patterns, with GCG maintaining strong network presence through 14 interactions (Figure 3C & (20 interactions) correlating with extensive biological process involvement, showing maximum counts (15) across metabolic processes, stimulus response, and biological regulation (Figure 4A). This aligns with research 37 demonstrating PPARG's crucial role in modulating multiple synchronized glucose homeostasis regulation³⁹. *A. bunius* showed moderate but significant enrichment (13 counts) across (Table 1). The significance of these degree values is supported by network biology principles, where nodes with higher degrees are considered hub proteins that play central roles in biological networks³². These hub proteins are particularly important as they typically represent essential components in biological processes, and their removal can significantly impact several pathways in the network^{33,34}. The varying degrees of connectivity across different proteins suggest species-specific mechanisms of action in their anti-diabetic properties, with higher degree values indicating more central roles in the therapeutic network^{35,36}, metabolic pathways including glycolysis and gluconeogenesis for glucose homeostasis. The network analysis revealed species-specific patterns complementing gene ontology findings. *S. cumini* exhibited GCG prominence (16 interactions)

reflected in robust biological process enrichment (15 counts) and membrane component distribution (15 counts) (

Figure 4 B). Recent studies ³⁸, showing that membrane-associated protein interactions enhance insulin secretion and glucose uptake mechanisms. *S. malaccense* demonstrated the highest enrichment (17 counts) in both metabolic processes and membrane components, corresponding with GCG and GCK's balanced connectivity (12 interactions each) (

Figure 4 C), indicating The analysis of gene ontology revealed sophisticated molecular mechanisms underlying the anti-diabetic properties of four medicinal plants. *C. myxa L.* demonstrated PPARG's

high connectivity (20 interactions) correlating with extensive biological process involvement, showing maximum counts (15) across metabolic processes, stimulus response, and biological regulation (

Figure 4 A). This aligns with research ³⁷ demonstrating PPARG's crucial role in modulating multiple synchronized glucose homeostasis regulation ³⁹. *A. bunius* showed moderate but significant enrichment (13 counts) across

Table 1: Predicted target genes associated to anti-diabetic metabolites derived from different plant species

Species	Gene	Degree	Closeness Centrality	Betweenness Centrality
<i>Cordia myxa L.</i>	PPARG	20	0.352631579	0.098385439
	PPARA	17	0.315294118	0.064317858
	RXRA	8	0.288172043	0.009811636
	GCG	16	0.30191458	0.076548946
<i>S. cumini</i>	SLC5A2	9	0.303703704	0.018722911
	DPP4	9	0.291607397	0.018942047
	GCG	14	0.349344978	0.123494994
<i>A. bunius</i>	SLC5A2	9	0.316831683	0.020780706
	DPP4	9	0.30651341	0.02297128
	GCG	12	0.338318	0.06800
<i>S. malaccense</i>	GCK	12	0.315881	0.06231
	SLC2A2	10	0.346743	0.02854

*The bolded proteins represent the selected targets for molecular docking, prioritized based on degree, closeness centrality, and betweenness centrality.

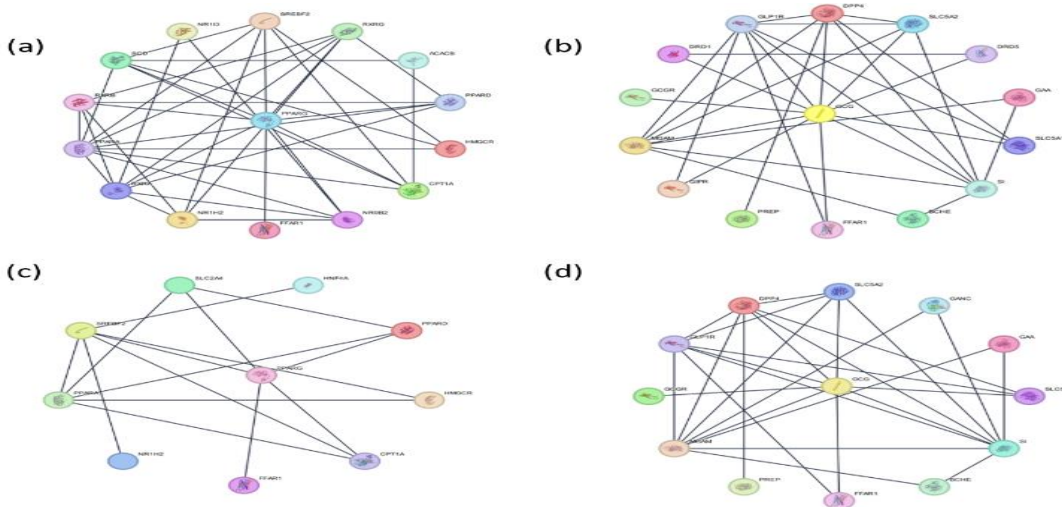


Figure 3: Protein-protein interaction (PPI) networks generated by the STRING database, demonstrating the antidiabetic activities associated with (a) *C. myxa*, (b) *S. cumini*, (c) *S. malaccense*, and (d) *A. bunius* plants.

categories, correlating with GCG's substantial network presence (14 interactions) (

Figure 4 D). The consistent enrichment of membrane-associated components across species supports research demonstrating six key mechanisms in diabetic syndrome amelioration, including enhanced insulin secretion and glucose uptake by muscle cells ³⁸.

The KEGG pathway enrichment analysis reveals intricate molecular mechanisms across the studied plant species, with notable correlations to their therapeutic potential. In *C. myxa*, the significant enrichment of PPAR signaling pathway (fold enrichment >60) aligns with its high STRING connectivity score for PPARG (20 connections) Figure 5 A), suggesting a robust role in metabolic regulation. This finding is supported by research demonstrating PPARG's crucial role in insulin sensitization and glucose homeostasis in type 2 diabetes treatment ⁴⁰. The adipocytokine signaling pathway enrichment further complements

this mechanism, as studies have shown its involvement in insulin resistance modulation through AMPK pathway activation. For *S. cumini* and *A. bunius*, the prominent enrichment in galactose and starch/sucrose metabolism pathways (fold enrichment ~60-100) correlates with their STRING network profiles, particularly GCG's high connectivity (16 and 14 connections respectively). This metabolic focus is consistent with research identifying their hypoglycemic properties through enhanced glucose uptake and metabolism (Figure 5 B & Figure 5 C) ⁴¹. The presence of carbohydrate digestion and absorption pathways in both species' enrichment profiles supports their traditional use in diabetes management ⁴². *S. malaccense*'s distinctive enrichment in PPAR and AMPK signaling pathways (fold enrichment 40-50) complements its unique STRING interaction profile where GCK and GCG show equal network strength (12 connections each). This dual mechanism is particularly noteworthy as recent studies have

demonstrated that simultaneous activation of these pathways can enhance insulin sensitivity and glucose uptake more effectively than single pathway targeting (Figure 5 D) ⁴³. The consistent presence of insulin resistance and glucagon signaling pathways across all species' enrichment profiles, albeit with varying significance levels, indicates a common underlying mechanism in their anti-diabetic properties, while their unique enrichment patterns suggest species-specific therapeutic approaches ⁴².

The molecular pathway analysis reveals intricate signaling networks governing metabolic regulation, as illustrated in the KEGG pathway diagrams. In the PPAR signaling pathway, ligand activation (including unsaturated fatty acids, eicosanoids, and NSAIDs) triggers PPAR-RXR heterodimer formation in three key tissues: liver, skeletal muscle, and adipose tissue. This complex regulates diverse target genes involved in ketogenesis (HMGCS2), lipid transport (ApoA1, ApoAV), fatty acid oxidation (ACO, CPT1, CPT2), and adipocyte differentiation (aP2,

ADIPOQ) (Figure 6) ³⁹. The pathway's tissue-specific effects are particularly evident in *C. myxa*, where PPARG's high connectivity (20 interactions) correlates with its enrichment score. The glucagon signaling pathway diagram demonstrates a complex interplay between multiple signaling cascades: cAMP signaling through CREB1, calcium signaling via IP3, and AMPK pathway activation (

Figure 7). This network shows how glucagon receptor activation influences glucose metabolism through key enzymes like PEPCK and G6Pase, while also modulating fatty acid oxidation through AMPK-mediated effects on acetyl-CoA carboxylase. The pathway diagrams reveal significant cross-talk through the AMPK signaling node, which integrates both PPAR and glucagon effects on metabolic regulation. This integration explains the observed synergistic effects in *S. malaccense*, where

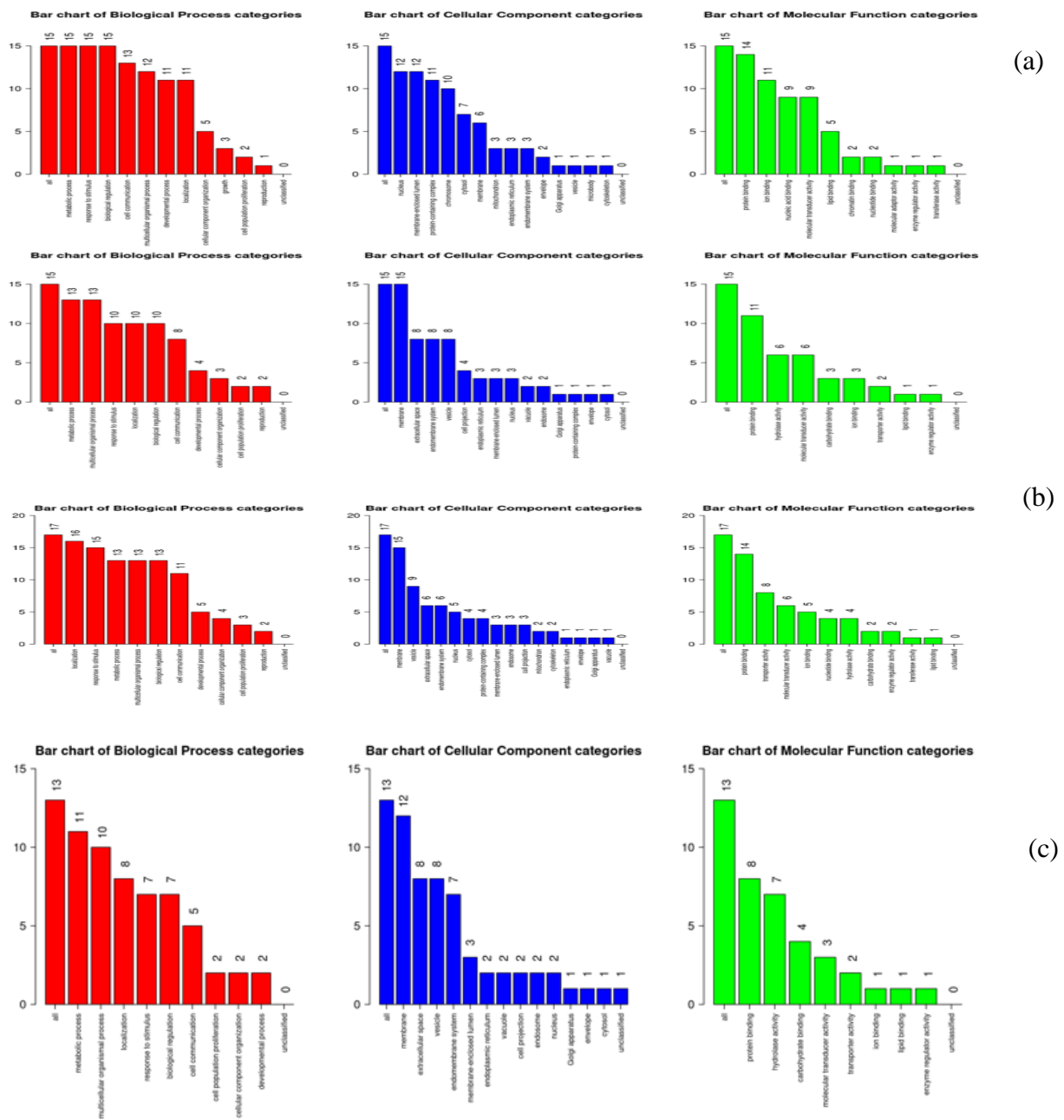


Figure 4: Gene Ontology Enrichment Analysis Showing Biological Processes (Red), Cellular Components (Blue), and Molecular Functions (Green) for (a) *C. myxa*, (b) *S. cumini*, (c) *S. malaccense*, and (d) *A. bunius*

(d)

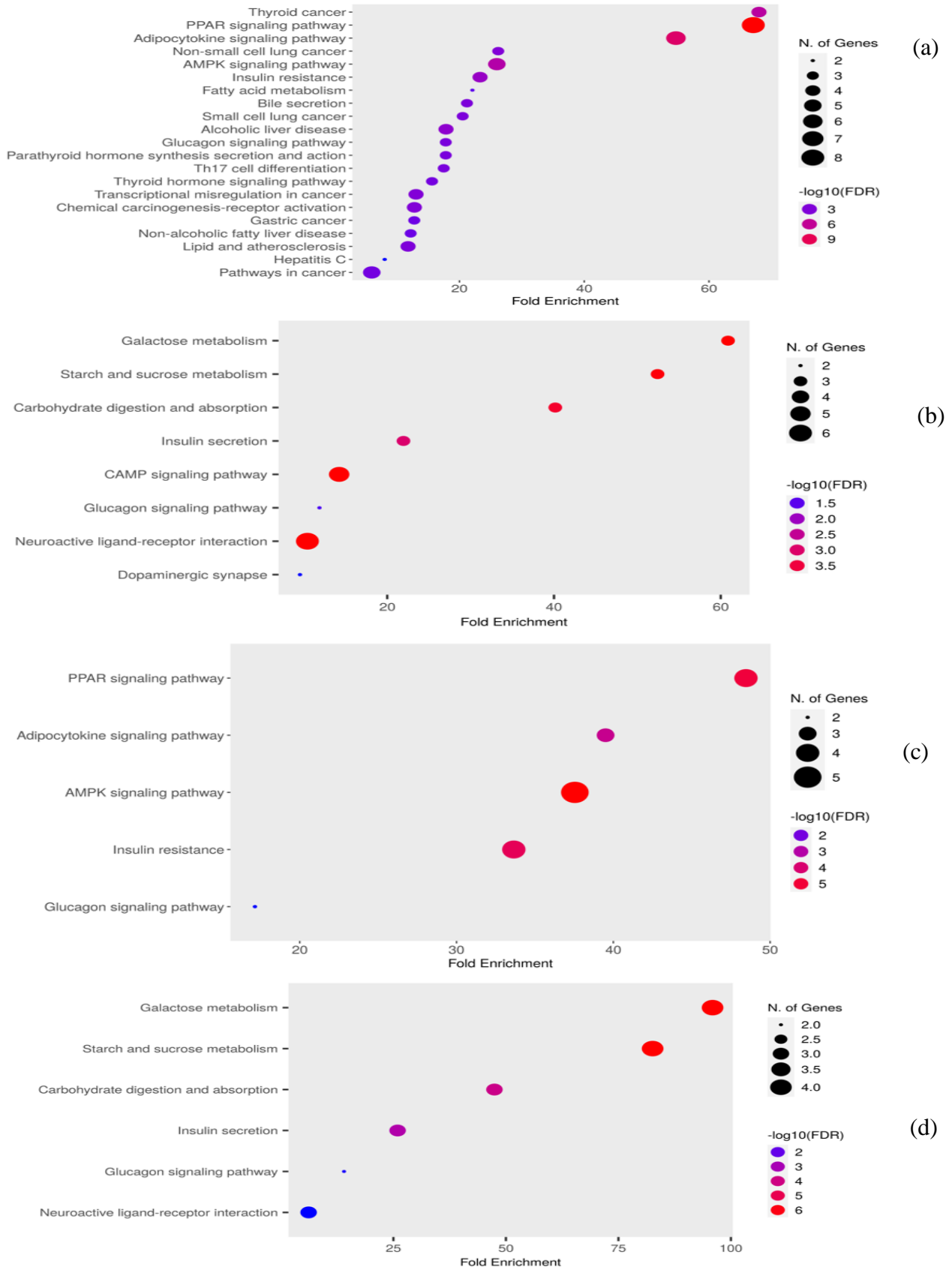


Figure 5: KEGG Pathway Enrichment Analysis Visualized as Bubble Plots for (a) *C. myxa*, (b) *S. cumini*, (c) *S. malaccense*, and (d) *A. bunius*, where Bubble Size Represents Pathway Enrichment and Color Intensity Indicates Statistical Significance

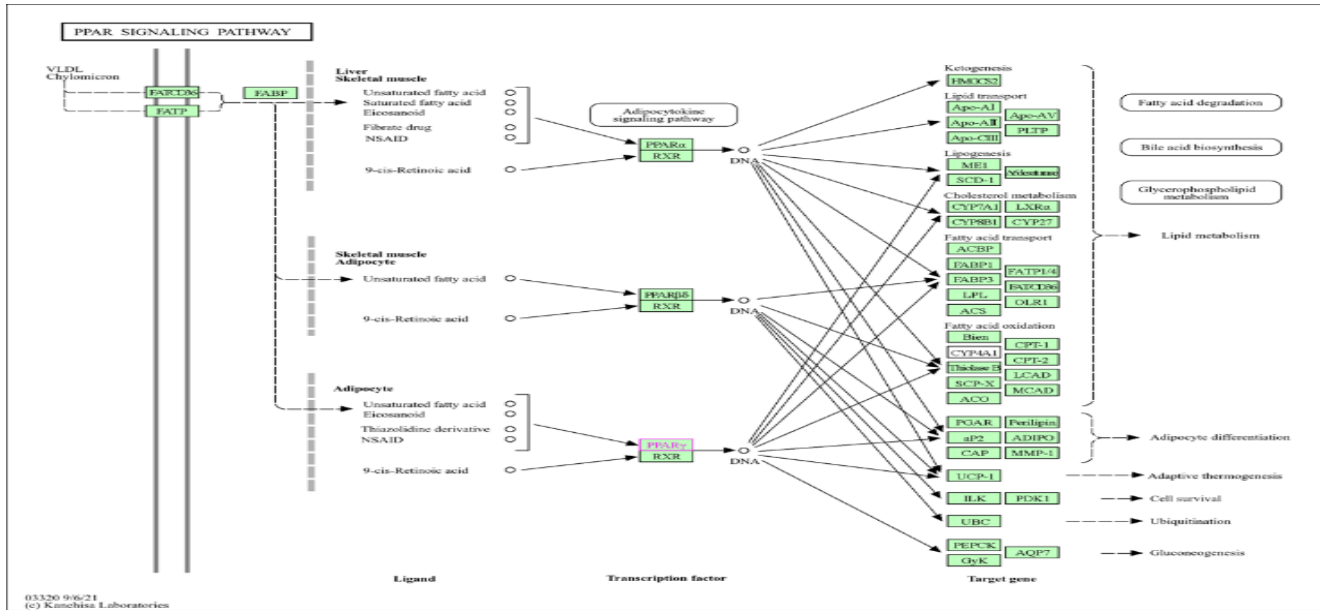


Figure 6: Molecular Mechanisms of Peroxisome Proliferator-Activated Receptor Gamma (PPAR γ) Protein Activity and Its Role in Diabetes Mellitus Pathogenesis

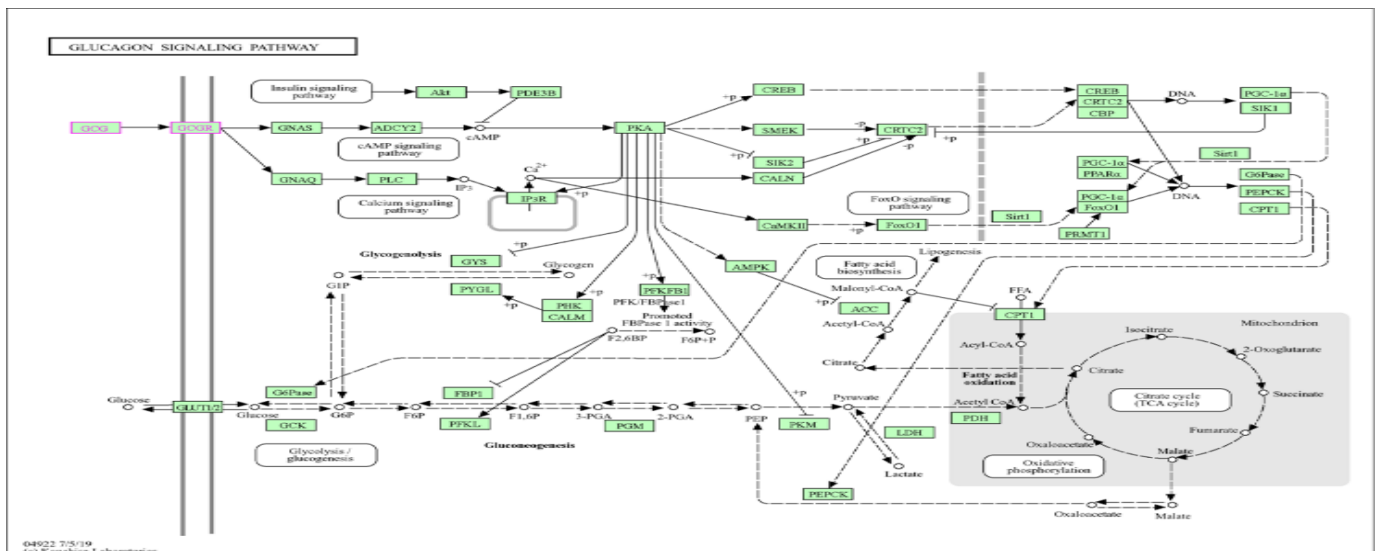


Figure 7: Signaling pathways involving Glucagon (GCG) protein activity and their role in the pathogenesis of diabetes mellitus.

balanced GCG and GSK activity (12 connections each) suggests coordinated metabolic control. The presence of multiple feedback loops and regulatory intersections, particularly in glucose homeostasis and lipid metabolism, provides molecular evidence for the therapeutic potential of targeting both pathways simultaneously in diabetes treatment, supporting the traditional use of these medicinal plants through well-defined molecular mechanisms³⁸⁻⁴⁰.

Molecular Docking

Since network pharmacology is employed to identify target proteins based on plant compound structures and their relationship to specific diseases, then molecular docking analysis is conducted to predict binding interactions between ligands and proteins at the molecular level, with initial binding site recognition being crucial for accurate results. The PPARG protein (PDB ID: 5YCP) utilizes Rosiglitazone as its natural ligand and positive control, functioning as a selective PPAR- γ agonist that plays a crucial role in regulating insulin-responsive genes. The activation of PPAR- γ enhances insulin sensitivity in adipose tissue, skeletal muscle, and liver, subsequently reducing blood glucose levels and endogenous glucose production⁴⁴. Prior study has demonstrated that Rosiglitazone exhibits anti-inflammatory properties by decreasing

NF- κ B transcription factor levels, which helps reduce systemic inflammation commonly observed in diabetic patients⁴⁵. However, significant cardiovascular side effects have been associated with Rosiglitazone use. Clinical studies have shown increased risks of heart failure, myocardial infarction, and cardiovascular death. Meta-analyses have revealed that Rosiglitazone usage can elevate heart attack risk by up to 30% compared to alternative treatments or placebos⁴⁵. To mitigate these adverse effects, *C. myxa* plant compounds were investigated using molecular docking to evaluate their potential in inhibiting diabetes mellitus pathogenesis. The study then expanded to include three additional plants targeting the GCG protein (PDB ID: 5EE7), utilizing MK-0893 as the native ligand. The molecular docking analysis encompassed both PPARG and GCG target proteins, aiming to identify compounds from the four selected plants with promising antidiabetic properties.

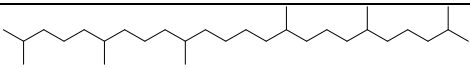
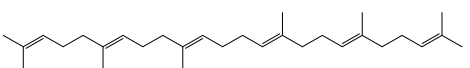
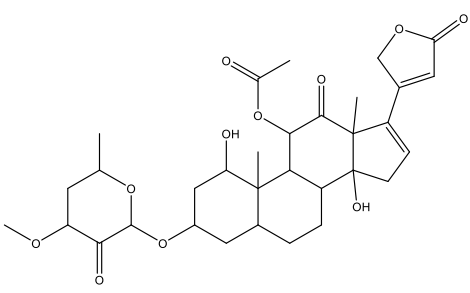
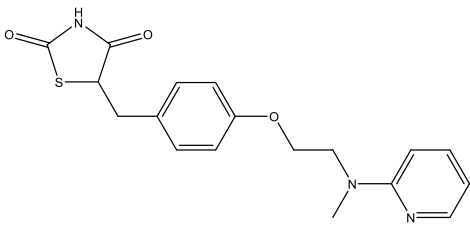
Molecular docking analysis revealed significant binding interactions between selected plant compounds and both PPARG and GCG receptors. For the PPARG receptor (PDB ID: 5YCP), three compounds from *C. myxa* demonstrated superior binding affinities compared to the standard drug Rosiglitazone (-7.49635 kcal/mol), with terpenoid

compounds of Squalane (-9.6078 kcal/mol), 2,6,10,14,18,22-Tetracosahexaene, 2,6,10,15,19,23-hexamethyl-(all-E)- (-8.7069 kcal/mol), and *Anodendroside G monoacetate* (-8.0845 kcal/mol) showing the strongest interactions. In the analysis of GCG receptor (PDB ID: 5EE7) interactions, *A. bunius* exhibited notable results from terpenoid compounds of 2,5,7,8-Tetramethyl-2-(4,8,12-Trimethyltridecyl)-3,4-Dihydro-2H-Chromen-6-Yl Hexofuranoside (-8.8001 kcal/mol), 2,6-Dimethyl-2-(4-methylpentyl)-3-(4-methylphenyl)-3H-chromen-4-one (-8.2000 kcal/mol), and 3-Hydroxy-2-(4-hydroxyphenyl)-5-methyl-4H-pyran-4-one (-7.9000 kcal/mol). For *S. malaccense*, the top docking score were also terpenoid compounds included 1,6,10,14,18,22-Tetracosahexaen-3-ol, 2,6,10,15,19,23-hexamethyl-, (all-E)- (-7.6398 kcal/mol),

2,6,10,14,18,22-Tetracosahexaene, 2,6,10,15,19,23-hexamethyl-, (all-E)- (-7.2562 kcal/mol), and 4-Hydroxy-3-methoxybenzaldehyde (-7.1208 kcal/mol). Lastly, *S. cumini* compounds showed promising binding with several terpenoids that are 2,6,10,14,18,22-Tetracosahexaene, 2,6,10,15,19,23-hexamethyl-, (all-E)- (-7.2562 kcal/mol), 5-(Geranyl/geranyl)-3,4-dihydroxybenzoic Acid (-6.983 kcal/mol), and 2H-1-Benzopyran-6-Ol, 3,4-Dihydro-2,7,8-Trimethyl-2-(4,8,12-Trimethyltridecyl)- (-6.5939 kcal/mol). This study highlighted the importance of terpenoid compounds as antidiabetic drugs, which is consistent with several reports regarding the effectiveness of terpenoids in treating diabetes⁴⁶⁻⁴⁸. The molecular interaction analysis PPAR γ reveals a well-positioned docking pose of Rosiglitazone with an RMSD value of 1.4004 Å (

Table 2), indicating high reliability of the docking results. The molecular interaction

Table 2: The top three docking results of *Cordia myxa* with PPAR γ receptor

Compound ID	Molecular name	Molecular Structure	S Score (Kcal/mol)
CM80	Squalane		-9.6078
CM69	2,6,10,14,18,22-Tetracosahexaene, 2,6,10,15,19,23-hexamethyl-, (all-E)-		-8.7069
CM44	<i>Anodendroside G</i> , monoacetate (CAS)		-8.0845
Native ligand (Rosiglitazone) (RMSD = 1.4004 Å)	Rosiglitazone		-7.49635

of the four ligands with PPAR γ reveals distinctive interaction patterns and binding characteristics. Rosiglitazone demonstrates the most specific interactions with the PPAR γ active site residues Gln286, Ser289, Ser314, His323, Lue330, Met364, and His449⁴⁹. Rosiglitazone, as native ligand exhibits the most specific and robust interactions, forming strong hydrogen bonds with Ser289, while also engaging with His449, Met364 and Leu330 (Figure 8 A), demonstrating its characteristic U-shaped conformation. Moreover, Squalene demonstrates limited interaction with the active site residues, primarily forming hydrophobic contacts with Met364 and Leu330 (Figure 8 B) without establishing specific hydrogen bonding networks.

Similarly, 2,6,10,14,18,22-Tetracosahexaene, 2,6,10,15,19,23-hexamethyl-, (all-E)- shows a predominant hydrophobic interaction pattern, engaging with Met364 and Leu330 through its extended hydrocarbon chain structure (Figure 8 C), while also forming non-specific contacts with surrounding hydrophobic residues. *Anodendroside G monoacetate* presents an intermediate interaction profile, where its acetate and hydroxyl moieties form hydrogen bonds with Cys285, Arg280, Gln273, and Ser274. At the same time, its steroid

scaffold establishes hydrophobic interactions with Met364 and Leu330 (

Figure 8 D), demonstrating a unique binding mode that combines both polar and non-polar interactions.

The Glucagon Receptor (GCGR) 's active site comprises complex amino acid residues that play pivotal roles in ligand binding and molecular recognition. The key residues Lys187, Tyr149, Ile235, Val191, Ile194, Met231, Glu362, and Phe365 form an intricate molecular environment that demonstrates

remarkable specificity and structural complementarity for ligand interactions⁵⁰. Our docking study The molecular docking analysis reveals a sophisticated landscape of ligand-protein interactions, where

Figure 9 A's MK-0893 native ligand (RMSD= 1.2772 Å) (dioxatetracyclo ligand extends the interaction diversity by revealing backbone acceptor interactions with Leu357, Pro356, and Val360, simultaneously connecting with

Figure 9 D is 1,6,10,14,18,22-Tetracosahexaen-3-ol through shared hydrophobic interaction mechanisms. The ligand's hydroxyl group engages with polar residues Ser350, Asn404, and Tyr343, while basic residues Lys349 and Arg346 create potential electrostatic interactions. Furthermore,

Figure 9 E's 4,4,6a,6b,8a,11,11,14b-Octamethyl-docosahdropicen-3-ol elaborates these interaction patterns by showcasing multiple hydroxyl groups interacting with Gln408 (Hydrogen bond) and Thr353, while

Figure 9 B's 2,5,7,8-

Figure 9 F's 2,6,10,14,18,22-Tetracosahexaene emphasizes hydrophobic residue

interactions with Leu403, Leu352, Leu329, and electrostatic interactions from Lys349, Lys405, and Arg346. Consequently,

Figure 9 G's 5-(Geranyl/geranyl)-3,4-dihydroxybenzoic acid introduces additional hydrogen bonding complexity through its carboxyl group's interactions with Lys405 and Asn404, and its 3,4-dihydroxy benzene ring engaging Ser350 and Lys349. Ultimately,

Figure 9 H's 2h-1-Benzopyran-6-Ol synthesizes these interaction mechanisms by demonstrating precise hydrogen bonding with Asn404 through its hydroxyl group, extensive hydrophobic stabilization by leucine residues, and potential π - π stacking interactions via Phe345.

Tetramethyl-2-(4,8,12-Trimethyltridecyl)-3,4-Dihydro-2h-Chromen-6-Yl Hexofuranoside, the interaction complexity intensifies with multiple hydrogen bonding points involving Ser350, Arg346, and Lys349, while maintaining a hydrophobic interaction network with leucine residues Leu347, Leu352, Leu399, and Leu403. Moreover, Figure 9 C's 7-Isopropyl-12-methyl-13-methylidene-2-aza-6,8-

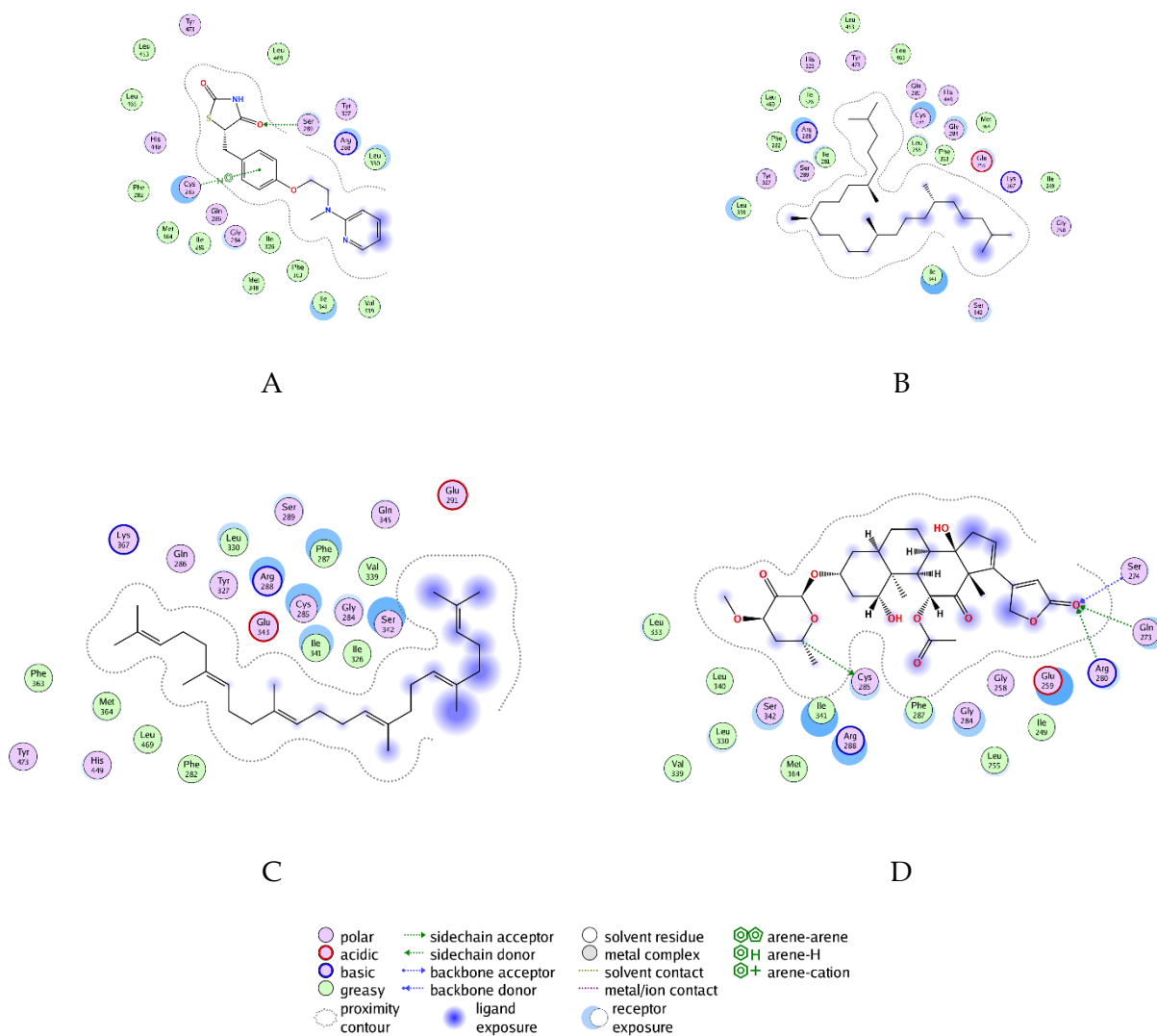


Figure 8: Molecular interactions of Rosiglitazone as Native ligand (A), and Squalane (B), 2,6,10,14,18,22-Tetracosahexaene, 2,6,10,15,19,23-hexamethyl-, (all-E)- (C), Anodendroside G, monoacetate (CAS) (D) against PPAR- γ as an antidiabetic agent

dioxatetracyclo ligand extends the interaction diversity by revealing backbone acceptor interactions with Leu357, Pro356, and Val360, simultaneously connecting with

Figure 9 D is 1,6,10,14,18,22-Tetracosahexaen-3-ol through shared hydrophobic interaction mechanisms. The ligand's hydroxyl group engages with polar residues Ser350, Asn404, and Tyr343, while basic residues Lys349 and Arg346 create potential electrostatic interactions. Furthermore,

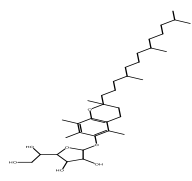
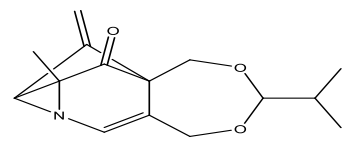
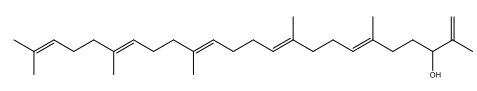
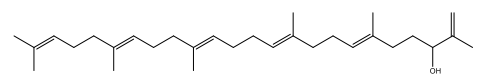
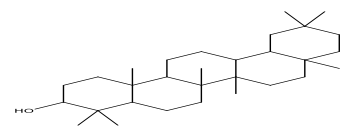
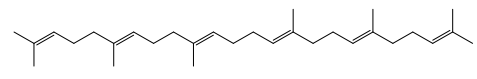
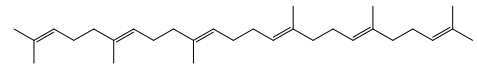
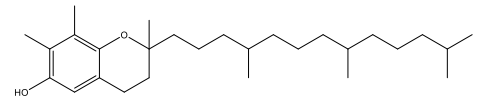
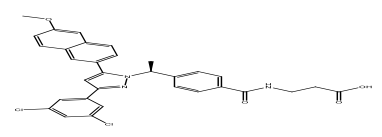
Figure 9 E's 4,4,6a,6b,8a,11,11,14b-Octamethyl-docosahydropicen-3-ol elaborates these interaction patterns by showcasing multiple hydroxyl groups interacting with Gln408 (Hydrogen bond) and Thr353, while

Figure 9 F's 2,6,10,14,18,22-Tetracosahexaene emphasizes hydrophobic residue

interactions with Leu403, Leu352, Leu329, and electrostatic interactions from Lys349, Lys405, and Arg346. Consequently, Figure 9 G's 5-(Geranyl/geranyl)-3,4-dihydroxybenzoic acid introduces additional hydrogen bonding complexity through its carboxyl group's interactions with Lys405 and Asn404, and its 3,4-dihydroxy benzene ring engaging Ser350 and Lys349. Ultimately,

Figure 9 H's 2h-1-Benzopyran-6-Ol synthesizes these interaction mechanisms by demonstrating precise hydrogen bonding with Asn404 through its hydroxyl group, extensive hydrophobic stabilization by leucine residues, and potential π - π stacking interactions via Phe345.

Table 3: Top Three Molecular Docking Conformations of Bioactive Compounds from *A. bunius*, *S. malaccense*, and *S. cumini* against GCG Receptor

Plants	Molecular name	Molecular Structure	S Score (Kcal/mol)
<i>A. bunius</i>			
AB94	2,5,7,8-Tetramethyl-2-(4,8,12-Trimethyltridecyl)-3,4-Dihydro-2h-Chromen-6-Yl Hexofuranoside		-8.8001
AB28	7-Isopropyl-12-methyl-13-methylidene-2-aza-6,8-dioxatetracyclo-[8.2.1.0(2,12).0(4,10)]tridec-3-en-11-one		-8.0234
AB52	1,6,10,14,18,22-Tetracosahexaen-3-ol, 2,6,10,15,19,23-hexamethyl-, (all-E)-		-7.6398
<i>S. malaccense</i>			
SM62	1,6,10,14,18,22-Tetracosahexaen-3-ol, 2,6,10,15,19,23-hexamethyl-, (all-E)-		-7.6398
SM71	4,4,6a,6b,8a,11,11,14b-Octamethyl-docosahydropicen-3-ol		-7.1208
SM52	2,6,10,14,18,22-Tetracosahexaene, 2,6,10,15,19,23-hexamethyl-, (all-E)-		-7.2562
<i>S. cumini</i>			
SC81	2,6,10,14,18,22-Tetracosahexaene, 2,6,10,15,19,23-hexamethyl-, (all-E)-		-7.2562
SC91	5-(Geranyl/geranyl)-3,4-dihydroxybenzoic Acid		-6.983
SC94	2h-1-Benzopyran-6-Ol, 3,4-Dihydro-2,7,8-Trimethyl-2-(4,8,12-Trimethyltridecyl)-		-6.5939
Native ligand (MK-0893) (RMSD = 1.2772 Å)	3-[[4-[(1~{S})-1-[3-[3,5-bis(chloranyl)phenyl]-5-(6-methoxynaphthalen-2-yl)pyrazol-1-yl]ethyl]phenyl]carbonylamino]propanoic acid		-5.66941

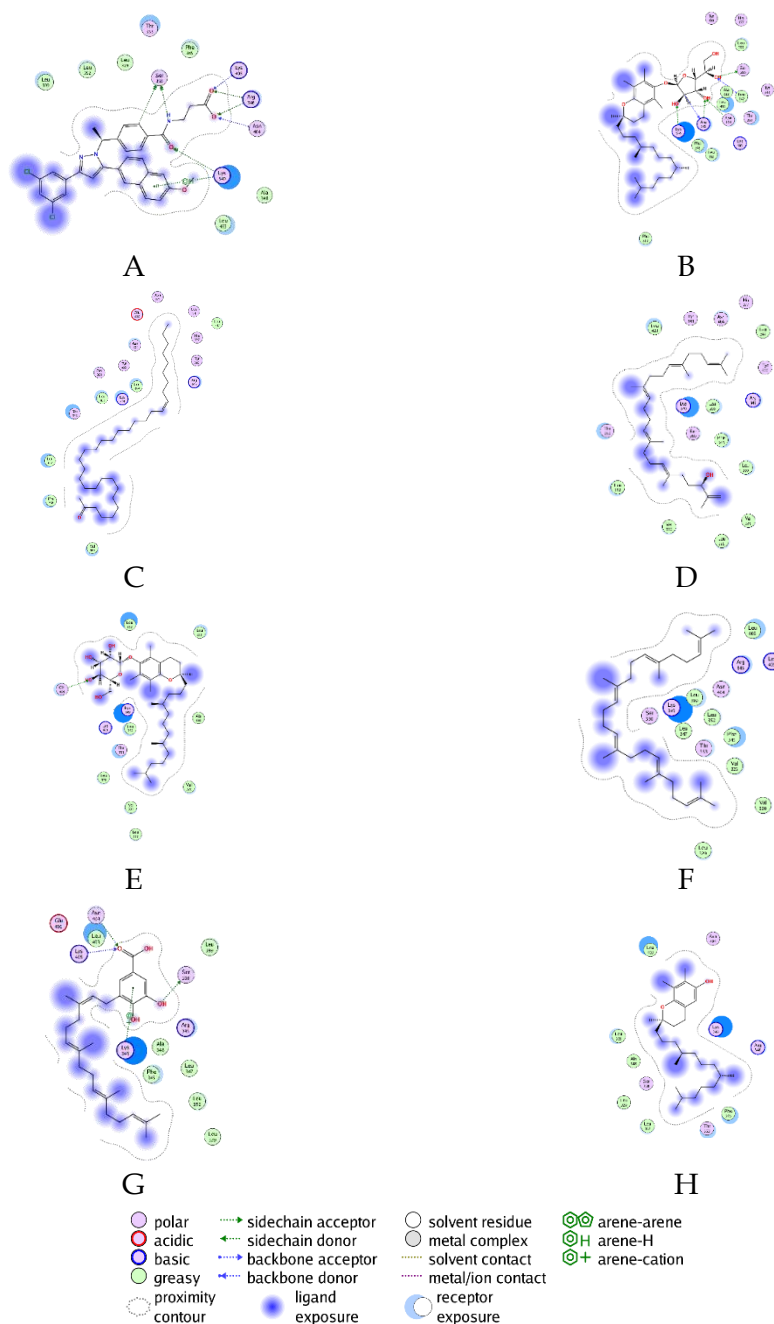


Figure 9: Molecular interactions of MK-0893 as Native ligand (A), 2,5,7,8-Tetramethyl-2-(4,8,12-Trimethyltridecyl)-3,4-Dihydro-2h-Chromen-6-Yl Hexofuranoside (B), 7-Isopropyl-12-methyl-13-methylidene-2-aza-6,8-dioxatetracyclo-[8.2.1.0(2,12).0(4,10)]tridec-3-en-11-one (C), 1,6,10,14,18,22-Tetracosahexaen-3-ol, 2,6,10,15,19,23-hexamethyl-, (all-E)- (D), 4,4,6a,6b,8a,11,11,14b-Octamethyl-docosahdropicen-3-ol (E), 2,6,10,14,18,22-Tetracosahexaene, 2,6,10,15,19,23-hexamethyl-, (all-E)- (F), 5-(Geranyl/geranyl)-3,4-dihydroxybenzoic Acid (G), and 2h-1-Benzopyran-6-Ol, 3,4-Dihydro-2,7,8-Trimethyl-2-(4,8,12-Trimethyltridecyl)- (H) against GCG as an antidiabetic agent

Conclusion

This study investigated the anti-diabetic potential of *C. myxa*, *A. bunius*, *S. malaccense*, and *S. cumini* using a multi-omics approach. GC-MS analysis revealed diverse metabolite profiles, combined with network pharmacology analysis demonstrated varying compound-gene interactions. Pathway enrichment analyses unveiled species-specific mechanisms: *C. myxa* in PPAR signaling, *S. cumini* and *A. bunius* in galactose and starch/sucrose metabolism, and *S. malaccense* in both PPAR and AMPK signaling pathways. Molecular docking analysis corroborated these findings, with compounds from *C. myxa*, particularly terpenoid of squalane, showing superior binding affinities to the PPARG receptor compared to Rosiglitazone. For the GCG receptor, terpenoids compounds from *A. bunius*, *S. malaccense*, and *S.*

cumini also demonstrated promising interactions. These results provide molecular evidence supporting the plants' traditional use in diabetes management, revealing diverse mechanisms of action. Limitations include lack of in vivo validation and limited pharmacokinetic analysis, suggesting future research should focus on in vivo studies, potential synergistic effects, and further investigation of pharmacokinetics and safety profiles to facilitate clinical application in diabetes treatment.

Conflict of interest

The author reports no conflicts of interest in this work.

Authors' Declaration

The authors hereby declare that the work presented in this article is original and that any liability for claims relating to the content of this article will be borne by them.

Acknowledgements

The authors acknowledge the Directorate General of Higher Education, Research, and Technology, Republic of Indonesia, for their financial support for this study under the grant scheme of strategic research collaboration (KATALIS) 2024 (contract number: Manual.1464/UN28.16/AL.04/2024).

References

1. Watcharachaisoponsiri T, Sornchan P, Charoenkiatkul S, Suttisansanee U. The α -glucosidase and α -amylase inhibitory activity from different chili pepper extracts. *Int Food Res J*. 2016;23(4):1439–1445.
2. Baynest HW. Classification, Pathophysiology, Diagnosis and Management of Diabetes Mellitus. *J Diabetes Metab*. 2015;6(5):1000541: 1-10
3. DiNicolantonio JJ, Bhutani J, O'Keefe JH. Acarbose: safe and effective for lowering postprandial hyperglycaemia and improving cardiovascular outcomes. *Open Heart*. 2015;2(1):e000327.
4. Najib A, Ahmad AR, Handayani V. ELISA Test on *Cordia myxa* L. Leaf Extract for alpha-Glucosidase Inhibitor. *Pharmacogn J*. 2019;11(2):358–361.
5. Najib A, Handayani V, Ahmad AR, Hamidu L, Anisa R. Chemoprofiling of active n-hexane fraction as alpha-glucosidase inhibitors from kanunang (*Cordia myxa* L.) leaves from enrekang south sulawesi. *J Glob Pharma Technol*. 2019;11(1):266–270.
6. Najib A, Handayani V, Ahmad AR, Hikmat S. Insilico screening chemical compounds α -glucosidase inhibitor from *Cordia myxa* L. *Int J Res Pharm Sci*. 2019;10(3):2054–2057.
7. Prema S, Sharma S, Kondrapu P, Kumre YM, Salim MR, Khatkar PK. Evaluation of antioxidant, antidiabetic and antihyperlipidemic activity of *Syzygium cumini* seeds in diabetic zebrafish model. *Eur Chem Bull*. 2023;12(6):2833–2839.
8. Akhtar J, Bashir F. Antidiabetic and Other Pharmacological Activities of *Syzygium cumini* (Black Plum or Jamun). 1st ed. CRC Press; 2023.
9. Nallappan D, Ong KC, Palanisamy UD, Chua KH, Kuppusamy UR. Myricetin derivative-rich fraction from *Syzygium malaccense* prevents high-fat diet-induced obesity, glucose intolerance and oxidative stress in C57BL/6J mice. *Arch Physiol Biochem*. 2023;129(1):186–197.
10. Tukiran T, Setiawan AR, Constat IC, Safitri FN. The Potency of Java Apple (*Syzygium samarangense*) AS α -Glucosidase and α -Amylase Inhibitor: An In-Silico Approach. *Trop J Nat Prod Res*. 2023;7(10):4124–4199.
11. Vadu S, Modi N, Prajapati M. A review on phytochemistry and traditional therapeutic benefits of *Syzygium malaccense* (L.). *Int Assoc Biol Comput Dig*. 2023;2(1):275–286.
12. Tayyeb A, Ashfaq I, Ambreen S. Mutagenic and Antimutagenic Potential of Fruit Juices of Some Medicinal Plants. In: *Biotechnologies and Genetics in Plant Mutation Breeding*. Apple Academic Press; 2023. p. 205–226.
13. Chowtivannakul P, Srichaikul B, Talubmook C. Hypoglycemic and Hypolipidemic Effects of Seed Extract from *Antidesma burius* (L.) Spreng in Streptozotocin-induced Diabetic Rats. *Pak J Biol Sci*. 2016;19(5):211–218.
14. Handayani V. Chemoprofiling of active n-hexane fraction as alpha-glucosidase inhibitors from Kanunang (*Cordia myxa* L.) leaves from Enrekang South Sulawesi. *J Glob Pharma Technol*. 2022;11(11):266–270.
15. Alseekh S, Aharoni A, Brotman Y, Contrepolis K, D'Auria J, Ewald J. Mass spectrometry-based metabolomics: a guide for annotation, quantification and best reporting practices. *Nat Methods*. 2021;18(7):747–756.
16. Chandran U, Mehendale N, Patil S, Chaguturu R, Patwardhan B. Network Pharmacology. In: *Innovative Approaches in Drug Discovery*. Elsevier; 2017. p. 127–164.
17. Ekowati J, Tejo BA, Maulana S, Kusuma WA, Fatmiani R, Ramadhanti NS, Norhayati N, Nofianti KA, Sulistyowaty MI, Zubair MS, Yamauchi T, Hamid IS. Potential Utilization of Phenolic Acid Compounds as Anti-Inflammatory Agents through TNF- α Convertase Inhibition Mechanisms: A Network Pharmacology, Docking, and Molecular Dynamics Approach. *ACS Omega*. 2023;8(49):15350–15360.
18. Zubair MS, Anam S, Khumaidi A, Susanto Y, Hidayat M, Ridhay A. Molecular docking approach to identify potential anticancer compounds from *Begonia (Begonia sp)*. In: *New York, NY, USA*; 2016. p. 0800051 - 0800057
19. Zubair MS, Alarif WM, Ghandourah MA, Anam S, Jantan I. Cytotoxic Activity of 2-O- β -glucopyranosil Cucurbitacin D from Benalu Batu (*Begonia sp*) Growing in Morowali, Central Sulawesi. *Indones J Chem*. 2020;20(4):766–778.
20. Zubair MS, Alarif WM, Ghandourah MA, Anam S. A new steroid glycoside from *Begonia sp*: cytotoxic activity and docking studies. *Nat Prod Res*. 2021;35(13):2224–2231.
21. Olaokun OO, Zubair MS. Antidiabetic Activity, Molecular Docking, and ADMET Properties of Compounds Isolated from Bioactive Ethyl Acetate Fraction of *Ficus lutea* Leaf Extract. *Molecules*. 2023;28(23):7717–7736.
22. Zubair MS, Maulana S, Widodo A, Pitopang R, Arba M, Hariono M. GC-MS, LC-MS/MS, Docking and Molecular Dynamics Approaches to Identify Potential SARS-CoV-2 3-Chymotrypsin-like Protease Inhibitors from *Zingiber officinale* Roscoe. *Molecules*. 2021;26(17):5230
23. Okafor CE, Ijoma IK, Igboamalu CA, Ezebalu CE, Eze CF, Osita-Chikeze JC, Uzor CE, Ekwuekwe AL. Secondary metabolites, spectra characterization, and antioxidant correlation analysis of the polar and nonpolar extracts of *Bryophyllum pinnatum* (Lam) Oken. *BioTechnologia*. 2024;105(2):121–136.
24. Jia C, Pan X, Wang B, Wang P, Wang Y, Chen R. Mechanism Prediction of *Astragalus membranaceus* against Cisplatin-Induced Kidney Damage by Network Pharmacology and Molecular Docking. *Evid Based Complement Alternat Med*. 2021;7(1):1–15.
25. Zhou P, Zhou R, Min Y, An LP, Wang F, Du QY. Network Pharmacology and Molecular Docking Analysis on Pharmacological Mechanisms of *Astragalus membranaceus* in the Treatment of Gastric Ulcer. Seidel V, editor. *Evid Based Complement Alternat Med*. 2022;2022:1–11.
26. Li F, Duan J, Zhao M, Huang S, Mu F, Su J, Liu K, Pan Y, Lu X, Li J, Wei P, Xi M, Wen A. A network pharmacology approach to reveal the protective mechanism of *Salvia miltiorrhiza-Dalbergia odorifera* coupled-herbs on coronary heart disease. *Sci Rep*. 2019;9(1):19343-19353.
27. Chen EY, Tan CM, Kou Y, Duan Q, Wang Z, Meirelles GV, Clark NR, Ma'ayan A. Enrichr: interactive and collaborative HTML5 gene list enrichment analysis tool. *BMC Bioinformatics*. 2013;14(1):128.
28. Liao Y, Wang J, Jaehnig EJ, Shi Z, Zhang B. WebGestalt 2019: gene set analysis toolkit with revamped UIs and APIs. *Nucleic Acids Res*. 2019;47(W1):W199–205.
29. Zhou Y, Zhou B, Pache L, Chang M, Khodabakhshi AH, Tanaseichuk O, Benner C, Chanda SK. Metascape provides a biologist-oriented resource for the analysis of systems-level datasets. *Nat Commun*. 2019;10(1):1523.
30. Ijoma IK, Okafor CE, Ajiwe VI. Computational Studies of 5-methoxypsoralen as Potential Deoxyhemoglobin S

- Polymerization Inhibitor. Trop J Nat Prod Res. 2024;8(10): 8835-8841
31. 31. Lee S, Oh DG, Singh D, Lee JS, Lee S, Lee CH. Exploring the metabolomic diversity of plant species across spatial (leaf and stem) components and phylogenetic groups. BMC Plant Biol. 2020;20(1):39.
 32. 32. Vazquez A. Protein interaction networks. Boca Raton: CRC Press; 2011. Chapter 8. PMID 21882453
 33. 33. Ochieng PJ, Hussain A, Dombi J, Kr sz M. An efficient weighted network centrality approach for exploring mechanisms of action of the Ruellia herbal formula for treating rheumatoid arthritis. Appl Netw Sci. 2023;8(1):53-82.
 34. 34. Wimalagunasekara SS, Weeraman JWJK, Tirimanne S, Fernando PC. Protein-protein interaction (PPI) network analysis reveals important hub proteins and sub-network modules for root development in rice (*Oryza sativa*). J Genet Eng Biotechnol. 2023;21(1):69-84
 35. 35. Zhang L, Shi X, Huang Z, Mao J, Mei W, Ding L, Zhang L, Xing R, Wang P. Network pharmacology approach to uncover the mechanism governing the effect of Radix *Achyranthis Bidentatae* on osteoarthritis. BMC Complement Med Ther. 2020;20(1):121.
 36. 36. Yao H, Xin D, Zhan Z, Li Z. Network pharmacology-based approach to comparatively predict the active ingredients and molecular targets of compound Xueshuantong capsule and Hexuemingmu tablet in the treatment of proliferative diabetic retinopathy. Evid Based Complement Alternat Med. 2021;2021(1):6642600.
 37. 37. Jacob B, Narendhirakannan RT. Role of medicinal plants in the management of diabetes mellitus: a review. 3 Biotech. 2019;9(1):4.
 38. 38. Alam S, Sarker MMR, Sultana TN, Chowdhury MNR, Rashid MA, Chaity NI, Zhao C, Xiao J, Hafez EE, Khan SA, Mohamed IN. Antidiabetic phytochemicals from medicinal plants: Prospective candidates for new drug discovery and development. Front Endocrinol (Lausanne). 2022;13:800714.
 39. 39. Chang CLT, Lin Y, Bartolome AP, Chen YC, Chiu SC, Yang WC. Herbal therapies for type 2 diabetes mellitus: chemistry, biology, and potential application of selected plants and compounds. Evid Based Complement Alternat Med. 2013;2013:378657.
 40. 40. Li L, Pan Z, Yang S, Shan W, Yang Y. Identification of key gene pathways and coexpression networks of islets in human type 2 diabetes. Diabetes Metab Syndr Obes. 2018;11:553-563.
 41. 41. Cui H, Hu D, Xu J, Zhao S, Song Y, Qin G, Liu Y. Identification of hub genes associated with diabetic cardiomyopathy using integrated bioinformatics analysis. Sci Rep. 2024;14(1):15324.
 42. 42. Zhong H, Duan BH, Du FM, Wang WM, Qiao H. Identification of key genes, biological functions, and pathways of empagliflozin by network pharmacology and its significance in the treatment of type 2 diabetes mellitus. Ann Transl Med. 2023;11(2):123.
 43. 43. Chen Chen, Minghui Han, Weimei Zhang, Jing Cui, Nan Cui, Lianzheng Cao, Guoqiang Luo, Jianping Sun. Identification of key genes and pathways in type 2 diabetes mellitus and vitamin C metabolism through bioinformatics analysis. Asia Pac J Clin Nutr. 2021;30(4):715-729.
 44. 44. Richter B, Bandeira-Echtler E, Bergerhoff K, Clar C, Ebrahim SH. Rosiglitazone for type 2 diabetes mellitus. Cochrane Database Syst Rev. 2007;(3):CD006063.
 45. 45. Xiu B, Xing A, Li S. The forgotten type 2 diabetes mellitus medicine: rosiglitazone. Diabetol Int. 2022;13(1):49-65.
 46. 46. Roy S, Ghosh A, Majie A, Karmakar V, Das S, Dinda SC, Bose A, Gorain B. Terpenoids as potential phytoconstituent in the treatment of diabetes: From preclinical to clinical advancement. Phytomedicine. 2024;129 (5):155638.
 47. 47. Putta S, Yarla NS, Kilari EK, Surekha C, Aliev G, Divakara MB, Santosh MS, Ramu R, Zameer F, Mn NP, Chintala R, Rao PV, Shiralgi Y, Dhananjaya BL. Therapeutic Potentials of Triterpenes in Diabetes and its Associated Complications. Curr Top Med Chem. 2016;16(23):2532-2542.
 48. 48. Song BR, Alam MB, Lee SH. Terpenoid-Rich Extract of *Dillenia indica* L. Bark Displays Antidiabetic Action in Insulin-Resistant C2C12 Cells and STZ-Induced Diabetic Mice by Attenuation of Oxidative Stress. Antioxidants (Basel). 2022;11(7):1227.